REPORT DOCUMENTATION PAGE

Form Approved
OMB No. 0704-0188

1. REPORT DATE *(DD-MM-YYYY)*	**2. REPORT TYPE**	**3. DATES COVERED** *(From - To)*
02-24-2010	Final Performance Report	01-01-2007 to 11-30-2009

4. TITLE AND SUBTITLE
Photorefractive Polymers for Updateable 3D Displays

5a. CONTRACT NUMBER
FA9550-07-1-0071

5b. GRANT NUMBER

5c. PROGRAM ELEMENT NUMBER

6. AUTHOR(S)
Nasser Peyghambarian
Robert A. Norwood

5d. PROJECT NUMBER

5e. TASK NUMBER

5f. WORK UNIT NUMBER

7. PERFORMING ORGANIZATION NAME(S) AND ADDRESS(ES)

Arizona Board of Regents,
University of Arizona
888 N. Euclid Ave., Room 510
Tucson, AZ 85721-0158

8. PERFORMING ORGANIZATION REPORT NUMBER

9. SPONSORING / MONITORING AGENCY NAME(S) AND ADDRESS(ES)

USAF, AFRL
AF Office of Scientific Research
875 N. Randolph St., Rm. 3112
Arlington, VA 22203

Office of Naval Research
San Diego Regional Office
4520 Executive Dr., Suite 300
San Diego, CA 92121-3019

10. SPONSOR/MONITOR'S ACRONYM(S)

11. SPONSOR/MONITOR'S REPORT NUMBER(S)

12. DISTRIBUTION / AVAILABILITY STATEMENT **Public Release**

13. SUPPLEMENTARY NOTES

14. ABSTRACT

During the tenure of this project a large area updateable 3D color display has been developed for the first time using a new co-polymer based photorefractive composite with fast writing times (ms), long persistence (hours) and rapid erasure time (several seconds) (*Nature* **45**, 694 (2008)). In order to enhance the recording speed of the holograms, a recording system with nanosecond pulsed laser having high repetition rate capable of writing the holographic pixel with single pulse was developed and the temporal response of the long-persistence photorefractive polymer composites was optimized to suit single nanosecond pulse exposure. A multi-color recording system was also developed and refreshable color holograms using photorefractive polymers have been demonstrated. Moreover, a 6 inch × 6 inch sample was fabricated demonstrating the feasibility of making large area 3D display devices.

15. SUBJECT TERMS

16. SECURITY CLASSIFICATION OF:			**17. LIMITATION OF ABSTRACT**	**18. NUMBER OF PAGES**	**19a. NAME OF RESPONSIBLE PERSON**
a. REPORT	**b. ABSTRACT**	**c. THIS PAGE**		26	Nasser Peyghambarian
					19b. TELEPHONE NUMBER *(include area code)* (520) 621-4649

Standard Form 298 (Rev. 8-98)
Prescribed by ANSI Std. Z39.18

Goals Accomplished:

(1) Developed TPD based photorefractive copolymers with image persistence of several minutes to hours.
(2) Developed holographic image recording set up to write and display 3D images.
(3) Demonstrated first updateable 3D display using photorefractive polymers
(4) Optimized the temporal response of the long-persistence photorefractive polymer composites to suit single nanosecond pulse exposure.
(5) A recording system with nanosecond pulsed laser having high repetition rate capable of writing the holographic pixel with one single pulse was developed.
(6) Developed multi-color recording systems
(7) Demonstrated a 4 × 4 inches, full parallax updateable holographic display that can be completed within 5 minutes.
(8) Fabricated 6 × 6 inches photorefractive updateable holographic display samples.

Holographic 3D displays provide highly realistic images without the need for special eyewear, making them valuable tools for applications that require "situational awareness" such as medical, industrial, and military imaging. A considerable amount of research has been dedicated to the development of three-dimensional (3D) imaging, as 2D images give only limited information about an object or a scene due to their lack of parallax and depth. 3D imaging techniques that rely on special eyewear such as polarizing goggles have unwanted side-effects such as eye fatigue and motion sickness and these systems are usually not suitable for more than one user. Holographic 3D displays are immune to these problems because they are viewable with the naked eye (autostereoscopic) by multiple users, and simulate natural human vision.

One of the major shortcomings of currently available holographic 3D displays is the static nature of the 3D images. These holographic displays employ photopolymers that lack image-updating capability, resulting in their restricted use and high cost. For defense applications (i.e. visualization of the battle space for mission planning and command-and-control) image-updating capability is a very important requirement as the battle space is a dynamic environment where the positions of the troops and military vehicles continuously change. Being able to visualize such changes in 3D is a significant advantage that would assist in mission planning, minimize causalities and reduce collateral damage. There are several technologies that allow real-time (dynamic) display of 3D images, unfortunately, they are static or require cumbersome eyewear.

Photorefractive (PR) polymers are dynamic holographic recording materials that allow updating of images, and have a wide range of applications including optical correlation, imaging through scattering media, and optical communication. To be suitable for 3D displays, photorefractive polymers need to have high diffraction efficiency, fast writing time, long image persistence, rapid erasure, and large area, a combination of properties that has not been shown before.

1. New photorefractive Co-polymer development and characterization

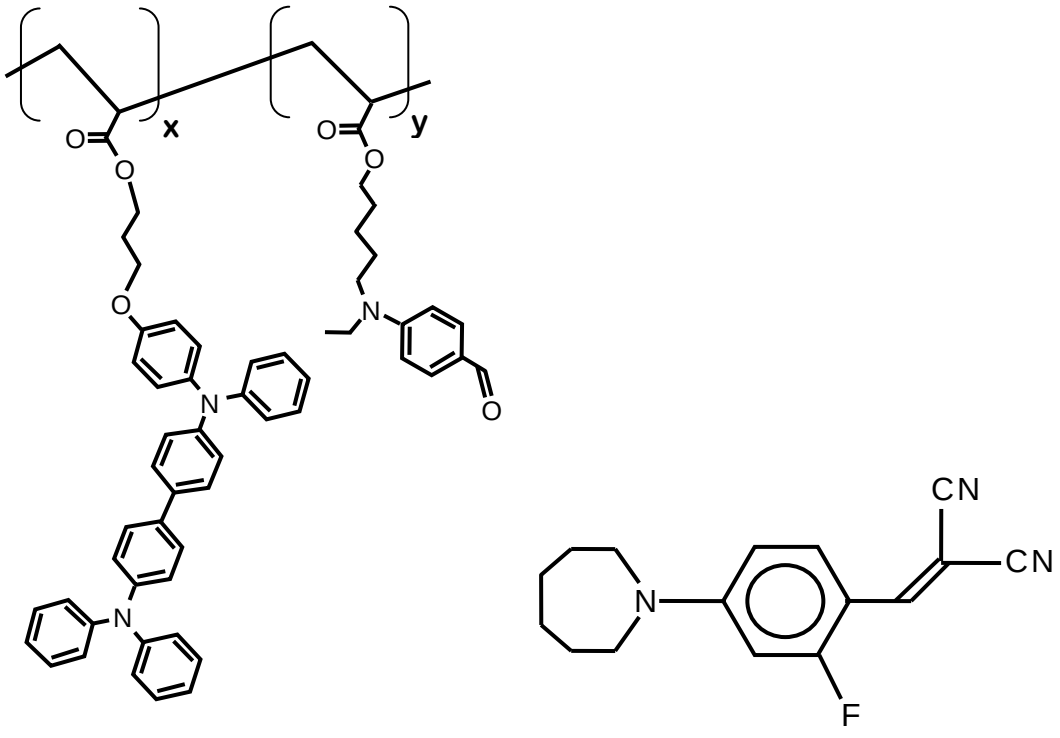

PATPD-CAAN F-DCST

Figure1. Chemical structures of the co-polymer (PATPD-CAAN) and the chromophore (F-DCST) used.

The new photorefractive polymer composites developed for 3D display applications contain a copolymer as the hole-transporting host matrix. The copolymer approach is followed to reduce the phase separation typical in guest-host polymer systems with low glass transition temperature (T_g), thus allowing increased loading of functional components such as NLO chromophores. The copolymer consists of a polyacrylate backbone with pendant groups tetraphenyldiaminobiphenyl-type (TPD) and carbaldehyde aniline (CAAN) attached through an alkoxy linker (PATPD-CAAN). A fluorinated dicyanostyrene (FDCST) NLO chromophore was added to provide sufficient refractive index change and charge generation at the wavelength of interest (532nm). The plasticizer N-ethyl carbazole (ECZ) was also used to reduce the T_g to room temperature. In some composites, a fullerene derivative [6,6]-Phenyl C61 butyric acid methyl ester (PCBM) was used to provide improved sensitization. Samples were prepared by melt processing a composite of PATPD-CAAN/FDCST/ECZ (50/30/20 wt%) (C1) between two indium-tin-oxide (ITO) coated glass slides. The thickness was set using glass spacer beads. Samples for nanosecond pulse writing were prepared with PCBM (C2= PATPD-CAAN/ FDCST/ECZ/PCBM (49.5/30/20/0.5 wt%)). Those samples used in the display showed no degradation or damage for several months over hundreds of write/erase cycles or showed no phase separation in an accelerated aging test at 60^0 C for 7 days.

The PR thin-film devices (C1) showed almost 90% diffraction efficiency at an applied voltage of 4kV using 532nm writing beams and a 633nm reading beam in a typical four-wave mixing (FWM) measurement (Fig1). Using the same irradiance, the two-beam coupling (TBC)

gain coefficient for the samples at 5kV is around 200cm^{-1}. Large area devices made of the composite showed no degradation or dielectric breakdown for extended periods of usage (several months) under very harsh conditions such as high applied fields and high power, focused laser beams.

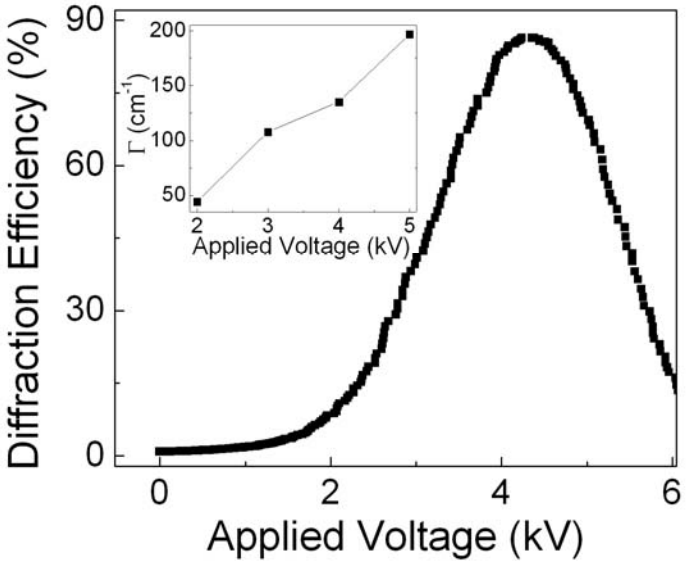

Figure 2. The steady state diffraction efficiency of the 100μm thick polymer composite is measured using writing beams at 532nm with a total irradiation of 1W/cm^2 and a reading beam at 633nm. Inset: Two-beam coupling gain vs. applied voltage.

The holograms recorded in the thin-film devices can persist for several hours in the dark (without writing beams) at an applied voltage of 4 kV while continuously being probed with a red (633nm) laser beam for which the samples are transparent. The total recording time of a 3D display that employs this material needs to be brought around a few minutes to achieve a high FOM. We have developed a new technique to improve the writing speed of organic PR materials based on manipulation of the applied voltage, which we call the "voltage kick-off". In conventional recording of PR polymers a fixed external voltage is usually applied across the polymer to pole the NLO chromophores. In the kick-off approach, we apply an increased voltage (i.e. 9kV) across the polymer to increase the writing speed during the hologram recording and then reduce the voltage to its optimum value of 4kV after recording is complete. The temporarily increased voltage facilitates efficient separation of electron-hole pairs and improves the drift characteristics forcing them to travel faster and increases the orientational order parameter and speed of the NLO chromophores. The reduction of the voltage to its optimum value after recording ensures hologram persistency. The overall benefit of the voltage kick-off is the reduction of the writing time per hologram to less than a second by fine tuning of the applied voltage (Fig 3). We have achieved a high diffraction efficiency of 55% with a total writing time of 0.5 second and several hours of hologram persistency in this composite using voltage kick-off.

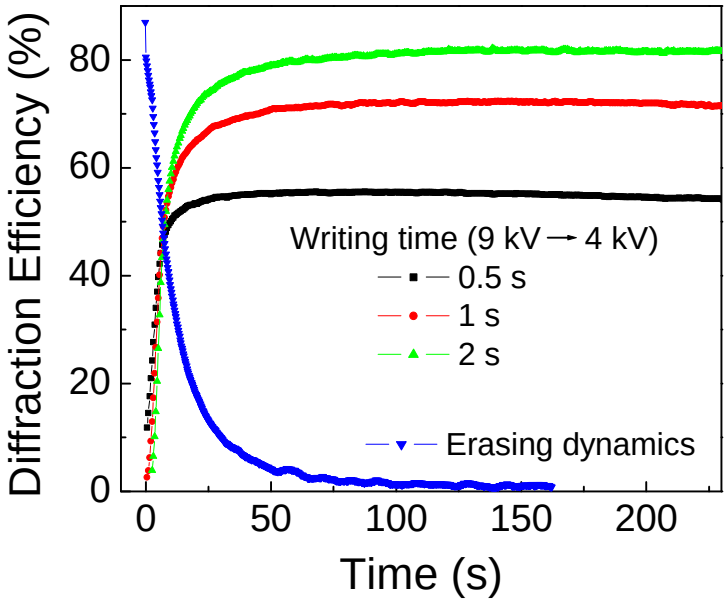

Figure 3. The writing beams at 532nm with 1W/cm^2 irradiance are turned on at an applied voltage of 9kV for a few seconds (writing time), and then turned off. After writing is complete, the voltage is reduced to 4kV to ensure hologram persistence and high diffraction efficiency. The diffraction efficiency increases in the dark (without writing beams) to its maximum value. The maximum diffraction efficiency achieved increases with the increasing writing time. Also shown is the erasing dynamics of the PR hologram at 9kV. The erasing beam is a spatially uniform 532nm laser beam at an irradiance of 1W/cm^2.

2. Holographic 3D display system

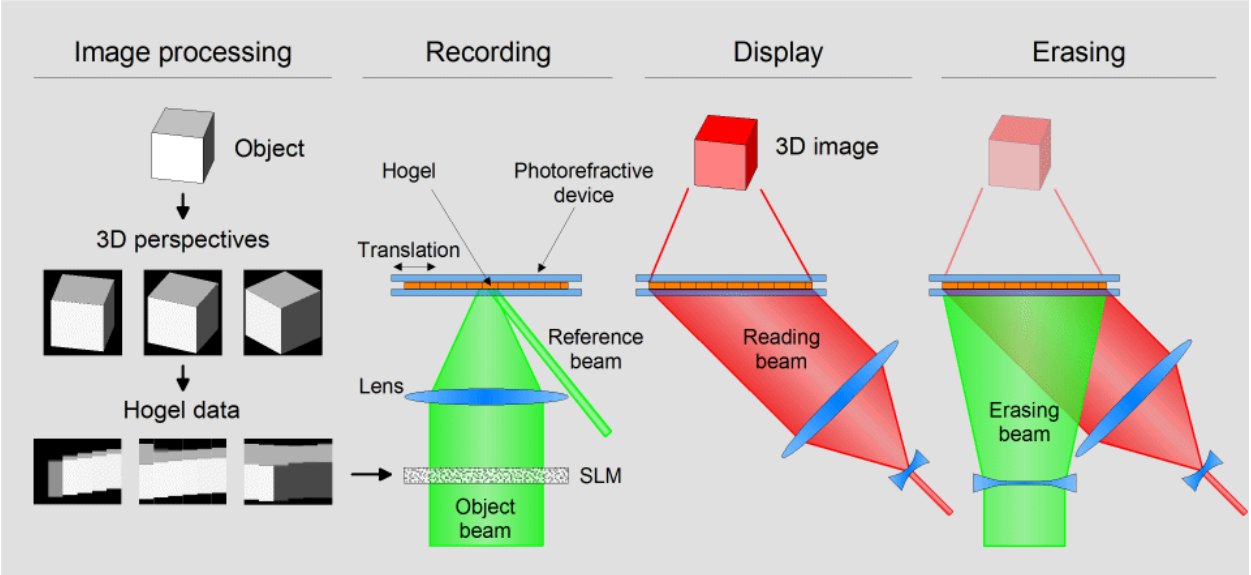

Figure 4. The 2D perspective views of the object are generated using a 3D computer model or a video camera moving on tracks around the object. The perspective images are re-organized (hogel data) and uploaded to the SLM. The SLM modulates the object beam, which is focused to the PR polymer and recorded in the Fourier transform geometry. The completed display can be viewed using a reading beam. The result is realistic 3D imagery with parallax and depth. The holograms can be erased by uniform illumination at the writing wavelength.

The hologram for 3D display is generated using integral image holography. Dozens of 2D perspectives of an object are processed on a computer and then optically multiplexed onto the recording medium in a manner such that when reconstructed, the sensation of depth is created via parallax (Fig.4). This allows a 3D image to be constructed from multiple 2D images without the real object ever needing to be present. A frequency-doubled Nd:YAG laser at 532nm is split into two paths, a reference beam and an object beam. The object beam is modulated using a spatial light modulator (SLM) with the image of a holographic pixel (hogel), constructed from the 2D perspectives. The reference beam is collimated and made to interfere in the sample with the object beam in a Fourier transform geometry. Given the geometry of the human vision, horizontal parallax only is used, so the object beam is only focused in this direction, creating hogels that are vertical stripes. The hologram is written by successively recording approximately 120 hogels side by side. The total writing intensity is approximately 100mW/cm^2. The writing time is limited by the response time of the sample and the vibration relaxation time of stage used to translate the sample, both of these being about 1s. The overall writing time is then 3-4 minutes for a 4inch × 4inch sample. After writing, the sample is translated to a new position and the hologram is read using a 650nm LED lamp. The low coherence length does not produce any speckle and the low absorption at this wavelength reduces de-trapping that causes the hologram to decay. Erasing can be done at any time by illuminating the sample with a homogeneous beam at the absorption band wavelength of 532nm. For the desired applications, it is beneficial to have a material that can be written quickly but decays very slowly. In order to facilitate this, we used voltage kick-off, in which typically 9kV is used during the writing to increase speed, while a decreased voltage typically 4kV is used for reading to increase persistency. For the degenerate four-wave mixing (DFWM), dynamics at 9kV it takes about 10s to reach 50% of its steady-state diffraction efficiency. However, an intermediate peak of approximately 10% is observed at the 1s mark. If at this time the writing beams are turned off and the voltage reduced to 4kV, the efficiency continues to increase in the dark. This is due to the fact that after approximately 1s of writing, the space charge field has been established, but the orientation time of the chromophores is longer, and will continue in the dark. This kick-off technique permits a hogel writing time of 1s in a material with a longer time constant.

We have recorded 3D displays (4× 4 inch in size) with complex and high quality images (Fig 5) within a few minutes using horizonatal parallax only (HPO) imaging. The 3D display exhibits a total horizontal viewing angle of 45 degrees. The Bragg mismatch usually observed in non-degenerate FWM that results in intensity variations across the horizontal view-zone is minimized by using a vertical reference/reading beam geometry. The images are viewable up to 3 hours directly on the photorefractive thin-film device without the need for intermediate projection tools or magnification between the recorded image and the viewer (Fig 5b). The images can be completely erased within minutes by uniform illumination of the display using a

532nm beam (Fig. 5c), and new images can be recorded when desired. There is no technological limit to the achievable display size, as large thin-film devices can be fabricated and even tiled together. For larger, full parallax displays a short pulsed recording can be employed, which is described in the following sections

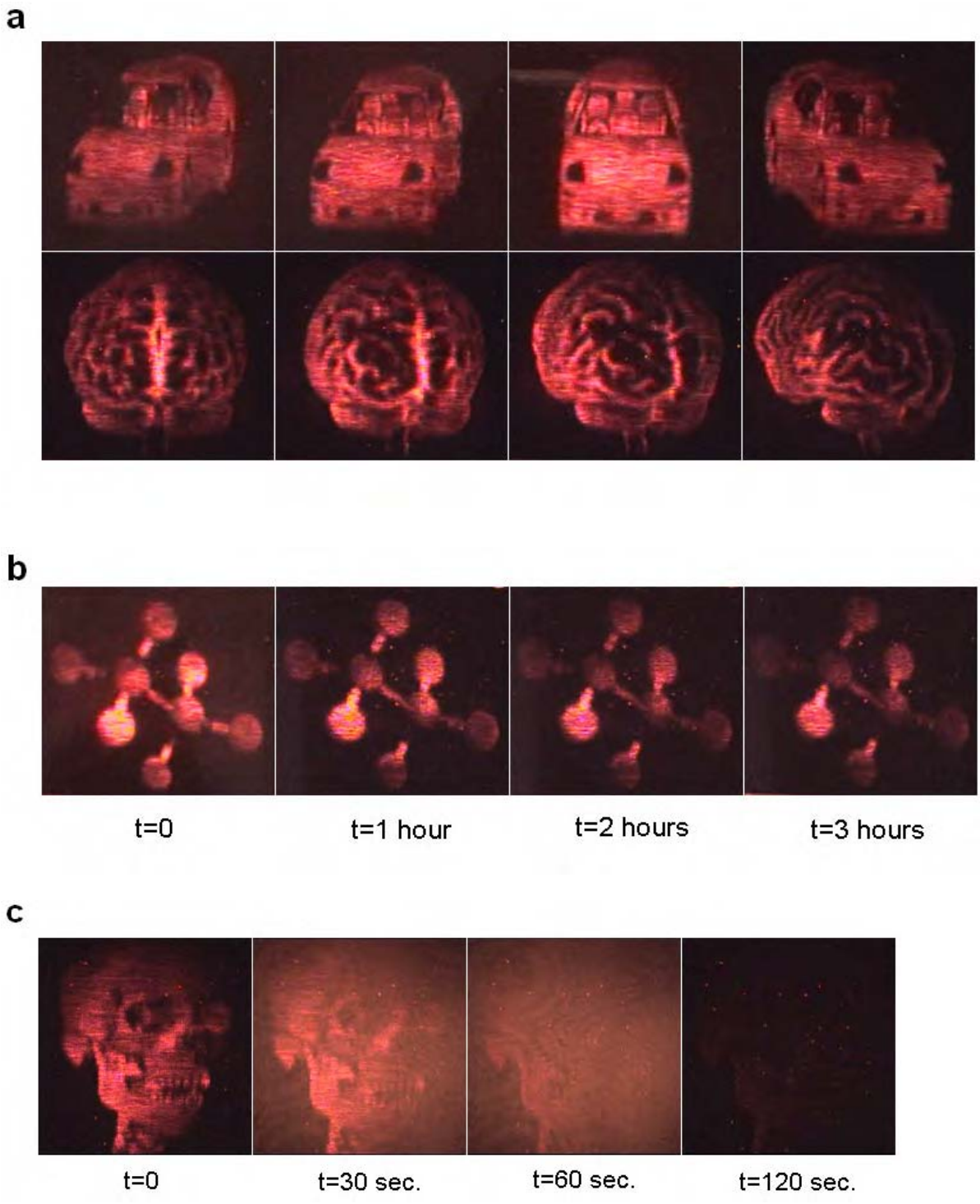

Figure 5. The display utilizes a single PR thin-film device with an active area of 4×4inches; (a) 3D hologram of a sports car was written, displayed, and then erased and a new hologram of a human brain was recorded onto the same area. The images were captured from a distance of 75cm from different angles to demonstrate the 3D effect using a video camera moving around the display. (b**)** The persistence of the hologram, in this case a 3D model of an ethane molecule is demonstrated by capturing pictures at different times after recording. The hologram is viewable for up to 3 hours without need for refreshing. (c) Erasure of a 3D image, a human skull, using uniform exposure is demonstrated. The hologram is completely erased in 2 minutes.

3. Faster recording systems

3.1 Increased CW laser power

With the initial writing laser source we used (5W Verdi from Coherent), the turnaround time for the write/erase cycle was 230 seconds (210+20) for a 4 × 4 inch sample. By using a more powerful laser (18W), we were able to reduce that time to 150 seconds (140+10) while maintaining the same diffraction efficiency.

The limiting factor in recording speed is no longer the writing time but the translation stage speed used in the set up and the settling time which accounts for 2/3 of the turnaround time; 100 seconds. Indeed, when increasing the cw laser power further and decreasing proportionally the recording time, the hologram diffraction efficiency is deteriorated (as seen in Fig. 6c). This reflects a fundamental technical limitation encountered when moving the sample rapidly and stopping it quickly due to induced vibrations in the setup during hologram recording.

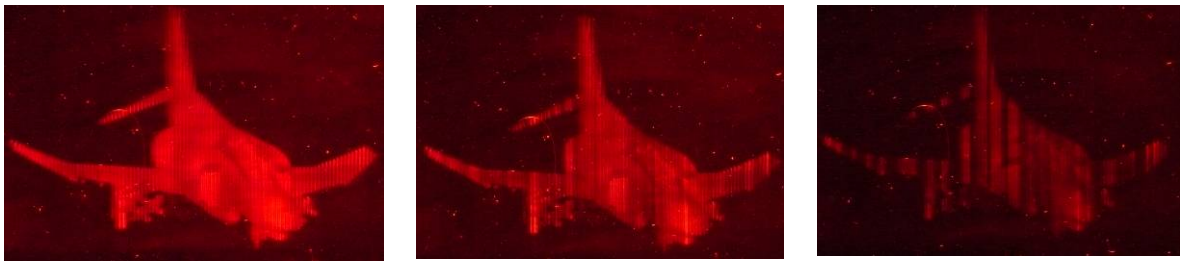

a) b) c)

Figure 6. Holograms were recorded with different power and writing time parameters: a) 5W, 1sec/hogel, 210 sec total, b) 15W, 0.45 s/hogel, 140 s total, c) 15W, 0.33 s/hogel, 130s total. Figure c shows how trying to further increase the recording speed decreases the diffraction efficiency due to translation stage vibration.

3.2 Single nanosecond pulse recording

While using a higher quality stage may improve the recording time, the ultimate solution is to use a nanosecond pulsed laser. Indeed, nanosecond pulse writing is insensitive to mechanical vibration and the stage can translate from one hogel position to the next at the repetition rate of the laser. The stage does not even need to stop during the recording.

In the single-shot pulsed exposure case, the two writing pulses create a light grating for the duration of the pulsewidth. The recording is almost instantaneous and hence vibration-free. The maximum diffraction efficiency, on the other hand, is created on the order of ~1-2ms due to the slow hopping charge transport mechanisms that prevail in polymers as well as chromophore orientation.

To test and develop this concept we installed a 100 Hz pulsed laser with 200 mJ/pulse power required to record a single hogel with each pulse (Innolas Hybrid). Power, beam profile, and coherence length have been certified together with the manufacturer. We demonstrated the recording of a diffraction grating with a single pulse in our copolymer photorefractive polymer (C2) material (Fig. 7). With these laser parameters, we should be able to reduce the recording time down to 1.2 second, a very big step towards realizing a real time 3D display.

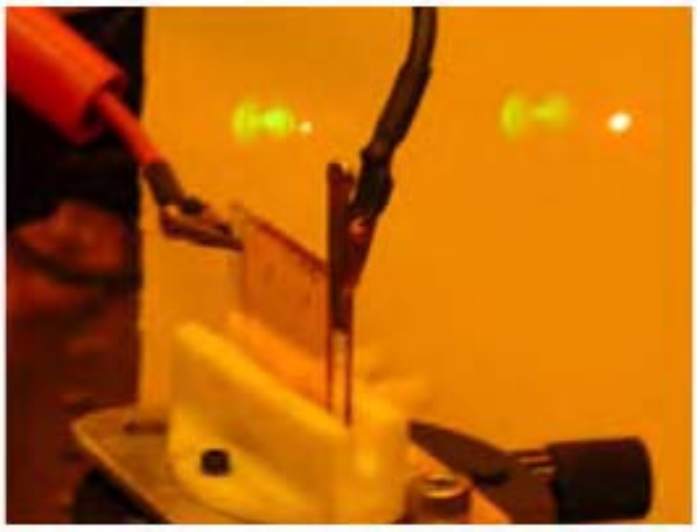

Figure 7. Single ns pulse four-wave-mixing. Both green spots are the writing beams from the pulsed laser. The right red spot is the zero order transmitted reading beam, and the left red beam is the diffracted beam.

4. Multi-color recording systems

To achieve a multi-color display, we have used angular multiplexing; two different holograms are written *at the same time* in the material at different angles. The recording angles were

selected to avoid crosstalk between the colors during readout and to achieve true color reconstruction at the observer location. To avoid unwanted interference between object beams, we have used two different techniques: polarization multiplexing and symmetrical geometry.

4.1 Polarization multiplexing

Polarization multiplexing is used to record both holograms at the same time without interference between object and reference beams of different holograms. The setup is shown in Figure 8. A 532 nm Nd:YAG laser is used as a coherent source for writing both holograms. The beam is split into an object and a reference beam. The object beam is expanded and separated according to the polarization before being sent to two different spatial light modulators. Each SLM imprints the information for one specific color. The two polarizations are then recombined by the same beam splitter element and horizontally focused by a cylindrical lens, forming a vertical line at the sample location. This line forms hogels and is two dimensional for horizontal parallax reproduction only.

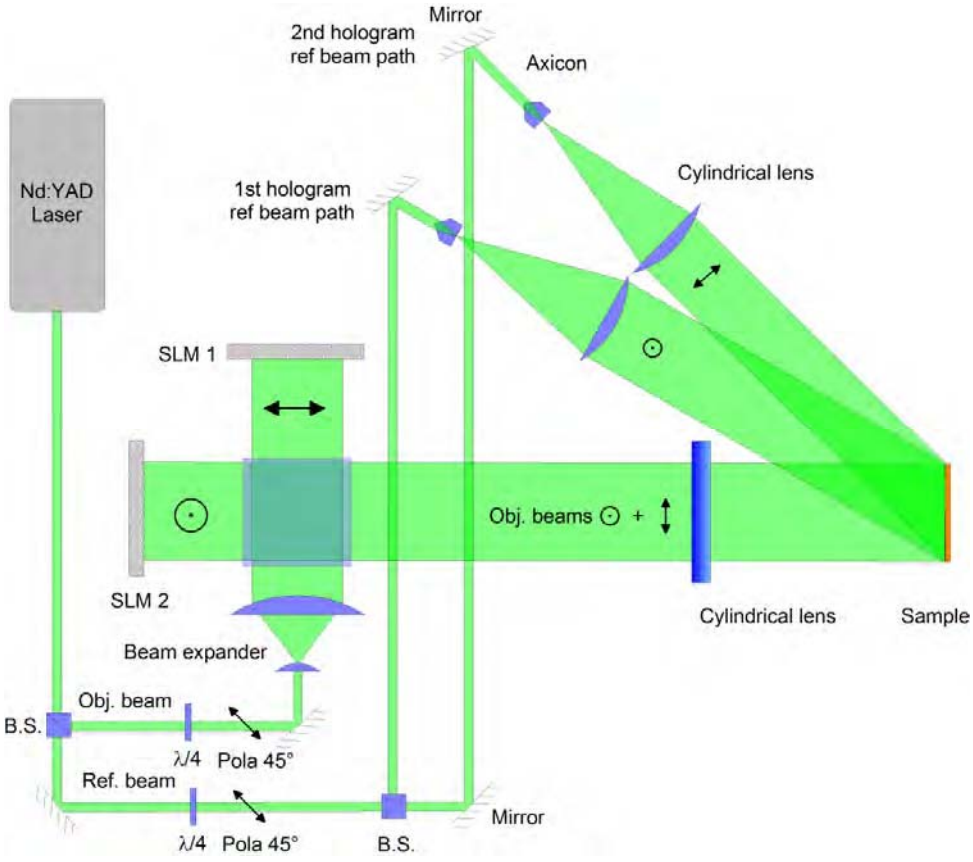

Figure 8. Side view sketch of the recording setup. B.S.: polarizing beam splitter, SLM: spatial light modulator. When recording, there are two reference and object beam pairs. They are orthogonally polarized so they do not interfere with each other. However, two holograms are recorded due to the interference between reference and object beams belonging to each pair. Each hologram will reconstruct a different color due to the difference of the reference beam angle.

For color encoding, there are two orthogonally polarized reference beams. Reference beam paths are composed of a microscope objective along with a cylindrical lens to generate a line. The angular difference between the reference beams has been carefully selected to avoid any color crosstalk when replaying the holograms, thus establishing true color replay at the observer location. Both pairs of reference/object beams have an orthogonal polarization so they do not interfere with each other. This permits recording of both holograms at the same time without any crosstalk, reducing the recording time, while maintaining the same diffraction efficiency.

White light is used to read the hologram (Fig. 9). Due to the angular multiplexing and wavelength separation, there is a view zone in which the true colors are diffracted toward the viewer. If the viewer moves vertically, the diffracted intensity decreases rapidly due to the Bragg selectivity.

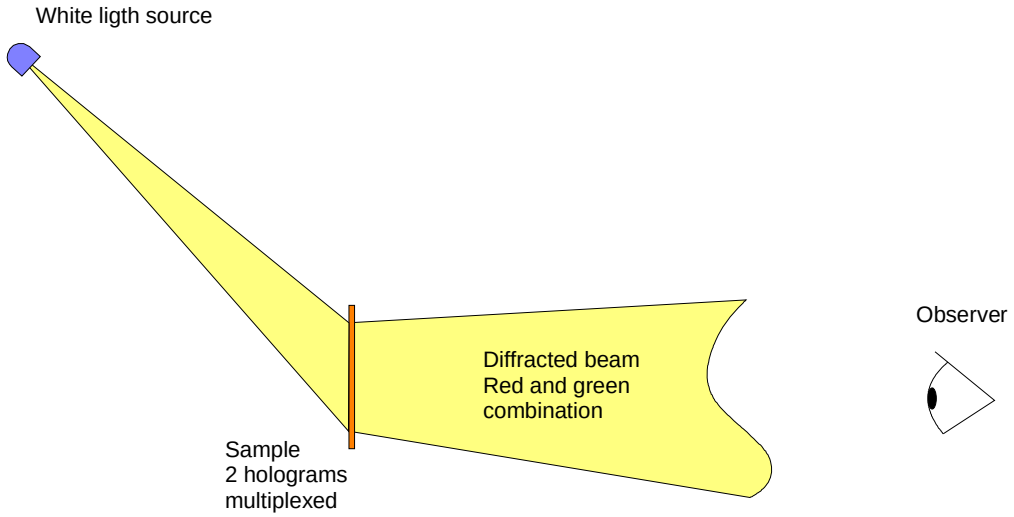

Figure 9. Reading geometry. A white light is used to read the multiplexed holograms. Each hologram diffracts the intended color to the observer location.

4.2 Symmetrical geometry

The other technique that has been investigated for color reproduction is based on the fact that the photorefractive organic material does not record gratings with the grating vector perpendicular to the external electric field. Therefore, two beams with their incident angles symmetric with respect to the sample normal will not give any diffraction. Hence, we used two object beams (coding red and green) having the same polarization but with their incident angle on opposite sides of the sample normal (Fig.10). There is only one reference beam, which is incident at an acute angle. Thus, there are three light intensity gratings, but only those from the object/reference beam pairs are recorded. The intensity grating generated by the interference between the two object beams does not result in any index modulation in the material. The hologram is read by two quasi-monochromatic light sources positioned at the Bragg angle and corrected for the difference between the recording and reading wavelengths (see Fig. 11). Practically, we use a red and a green light emitting diode to avoid speckle in the diffracted beam.

The color ratio is determined by the recording parameters and can be adjusted afterwards by adjusting the reading source intensity.

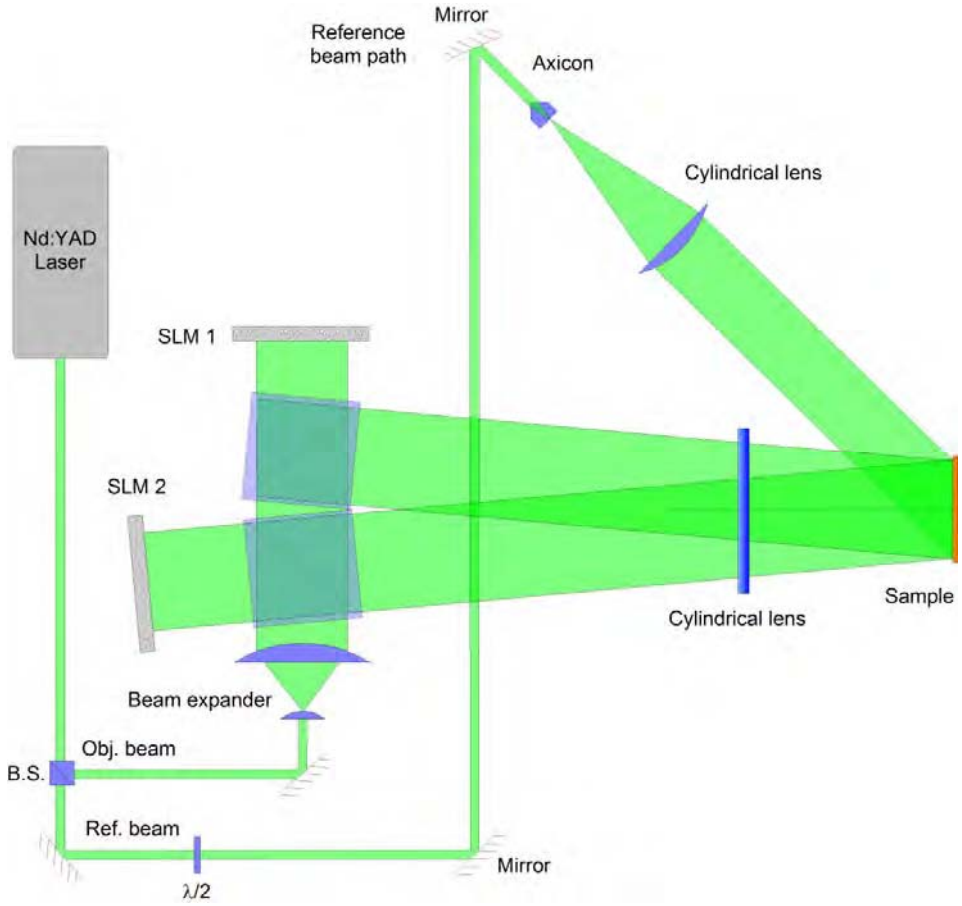

Figure 10. Color recording setup based on symmetry. Object beam angles are symmetrical with respect to the sample normal and there is only one reading beam. The interference pattern due to the interference of both object beams is not recorded in the sample due to the nature of the photorefractive process in polymers.

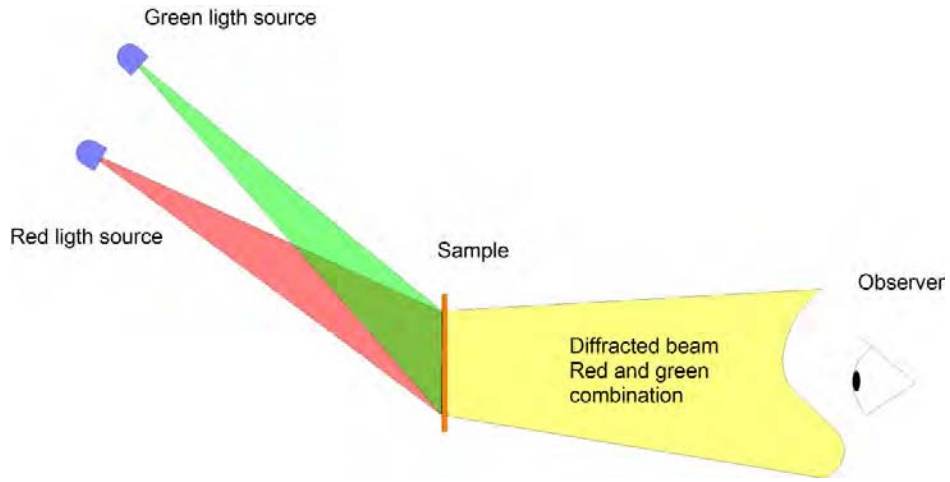

Figure 11. Reading geometry. When replaying the hologram, two light sources with different colors are positioned at their respective Bragg angles. Each hologram diffracts only one color and there is no chromatic crosstalk. The combination of the two diffracted beams recreates the object color.

It has to be noted that, even if this system is said to be "two colors", the observed hologram achieves multicolor operation based on the grey scale mix of the reading wavelengths. For the case of the polarization based system which uses white light for hologram readout, the wavelength selection is due to the Bragg selectivity.

If we look at the CIE chart (see Figure . 12), the colors that can be displayed are those included in the region joining both source spectra. Color sharpness is defined by the source spectrum extension and Bragg chromatic selectivity.

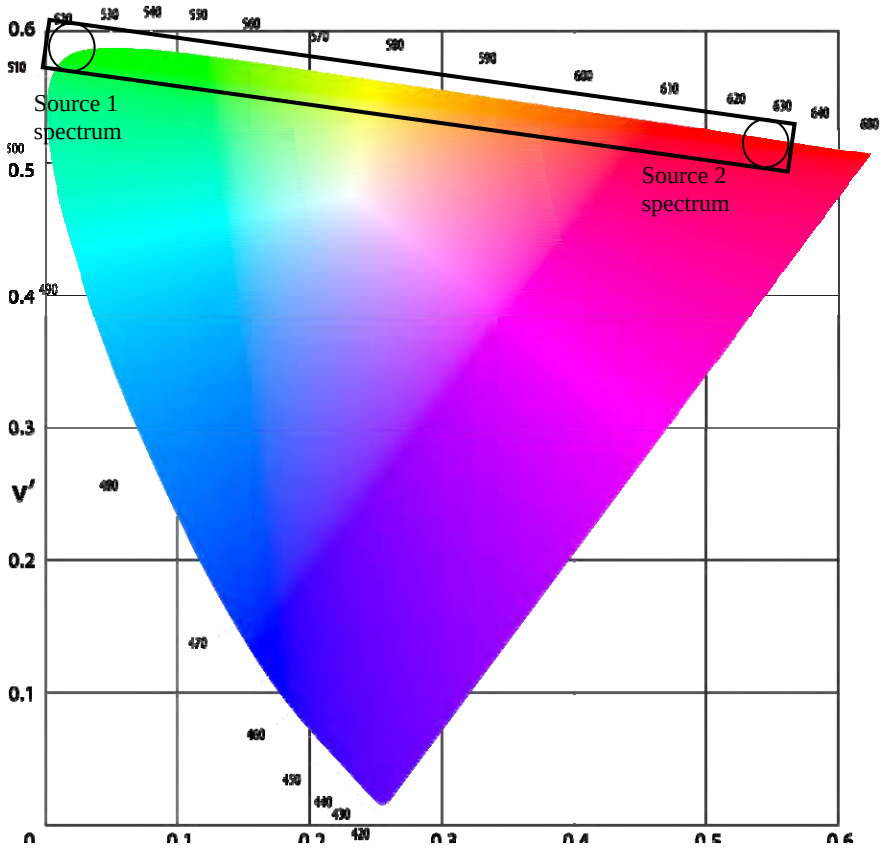

Figure 12. CIE diagram with the colors region accessible to the "2 color" 3D display. For sources color peak at 530 and 640 nm the accessible region include bright yellow.

4.3 Data encoding

As previously stated, we used holographic stereoscopy to reproduce the third dimension. This technique is based on optical multiplexing of a limited number of perspectives onto different parts of the display (Fig. 13.a). This technique permits reproduction of images with horizontal parallax, greatly reducing the amount of information and calculation compared to that needed for full parallax. For a color display, since holograms are independent, the color channels of the 2D perspective views are first split (Fig. 13.b). Then, each independent grey scale map is processed into hogel data by an integral photography algorithm (Fig. 13.c).

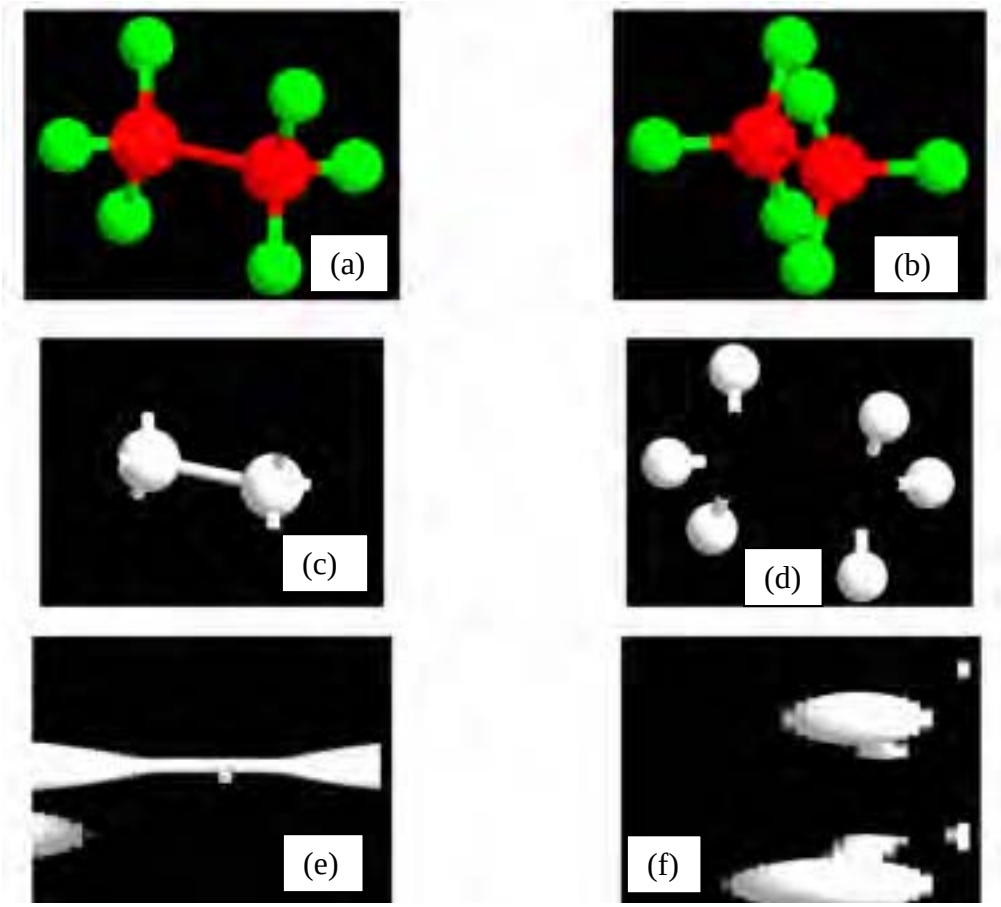

Figure 13. Hogel data generation for a color hologram. a, b: 2D perspectives of the object. c, d: Color channel dissociation. e, f: Hogel data. To generate the hogel data from a colored image, color channels are first split from each 2D perspective. Then each set of images is converted into hogel data using an integral photography algorithm.

The recorded hologram is erased by illuminating the whole surface of the sample with light whose wavelength is within the sensitivity region of the material. The erasure time depends on the wavelength and intensity. Although the erasing light does not need to be coherent, we used 532 nm laser light because of its power and its ready availability. Complete erasure of the hologram is achieved within a minute and the media is immediately ready for recording a new hologram.

We have written, erased and updated several different color holograms in a 6"× 6", 100μm thick sample. The number of hogels per color and per hologram was 120. The recording total irradiance (sum of both beams) was 0.1 W/cm².

Figure 14 shows an example of a multicolored hologram recorded with our system and captured with a digital camera. Here we can clearly see the ability of this technique to both capture brilliant pure colors (note the reds and greens) as well as arbitrary combinations thereof,

as observed in the gold vase. Note that the data encoding operation can easily be generalized to the three fundamental colors, enabling the generation of full color holograms.

Figure 14. Example of two color holograms. Compared to our previous technique, we see that the color hologram efficiency is higher, colors crispier and color mixing smoother. One can see how the vase is uniformly gold due to the combined diffraction of the green and red holograms.

5. Design of a full parallax system

It is know that a full parallax setup is easier to make than its horizontal parallax only (HPO) counterpart. Indeed there is no need to anamorphically format the writing beams with cylindrical lenses, spherical aberration corrected lenses can be used. However, a full parallax system requires a much larger number of hogels to be recorded. Compared to HPO, the number of hogels required for full parallax at the same resolution is squared factor, as is the recording time. For example, for a 4" × 4" sample, the number of hogels required for full parallax is 120^2 = 14,400. So, the recording time becomes an unreasonably large 240 minutes, which is more than the persistency time of the first hogels.

Full parallax display is enabled by the increased speed of pulsed laser recording. In this case the speed is determined by the laser repetition rate. At the 100Hz speed of the actual system, the recording time for our example becomes 144 seconds, about the same as that currently required for an HPO hologram written with a CW laser.

Nevertheless, larger samples will require a rapidly increasing number of hogels and the present systems will saturate quickly; for our goal of 1' × 1' sample, the recording time can be calculated to be 1,300 seconds (21 minutes) for a 100 Hz pulsed laser. To overcome this situation, we propose to reduce the hogel data resolution (currently higher than eye resolution, anyway) and write multiple hogels per shot. To do so, a micro-lenslet array can be used to focus the object beam while a holographic element plate will redirect the reference beam. The screen in front of the sample will be a perforated matrix, with holes the size of the hogels. During recording, the sample is raster scanned to cover the full matrix sub-element and then the full sample surface. A schematic of this design is presented in Figure 15.

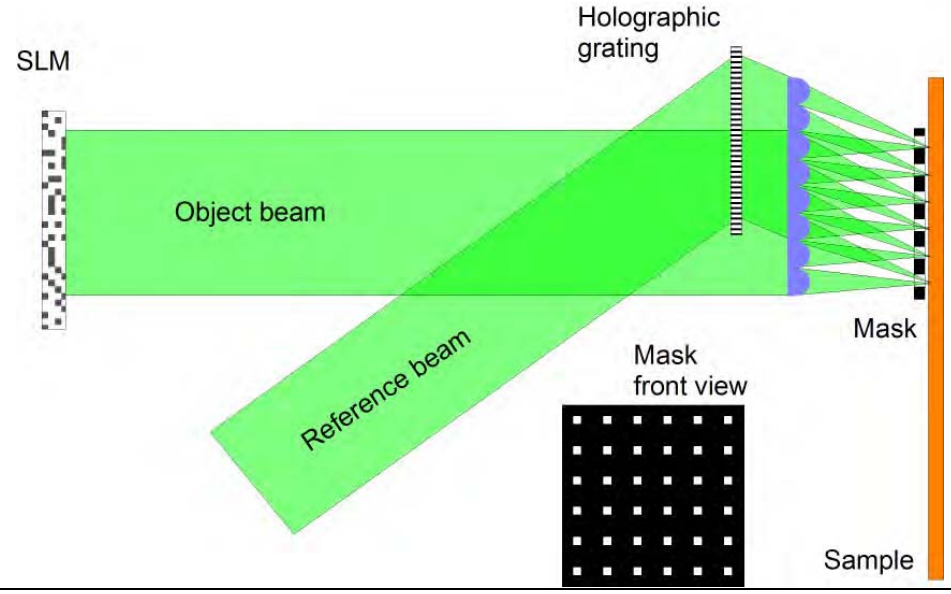

Figure 15. Schematic of the full parallax sub-aperture system. The holographic grating redirects the reference beam while letting the object beam pass through. The lenslet array focuses the beams in the sub-aperture defined by the mask. The translation stage moves the sample so that its surface is fully recorded.

The primary limitation of this approach is the division of the SLM resolution and the writing beam intensity by the number of sub elements, effectively limiting the number of apertures that can be used. There exist SLMs with higher resolution than the ones we are using now (HD TV vs VGA) but the high power pulsed laser system we currently employ is already near the state-of-the-art. This is why it is important to concurrently pursue research for increasingly sensitive photorefractive polymer materials that will require less energy to be recorded. If a suitable photorefractive polymer sample is developed with a 10 times improved sensitivity, we can use a low power pulsed laser as a writing source. Those lasers, based on diode pumping (diode pumped solid state - DPSS) as opposed flash lamps, can achieve a repetition rate of 100 kHz, improving the writing speed by a factor of 1,000. There will certainly be other engineering challenges at that speed, but this brings the whole concept close to a video rate holographic display.

6. Larger holograms

Increasing the size of the display is one of our priorities. The current display utilizes a 4 × 4 inch sample and the setup was adapted to record a hologram that size. Going for a larger display require several modifications:

- Larger samples
- Multi-row recording
- Increased laser power

6.1 Larger samples

A significant effort has been made to manufacture larger samples. 6 × 6 inches samples have been successfully produced, doubling the display surface (see figure 16).

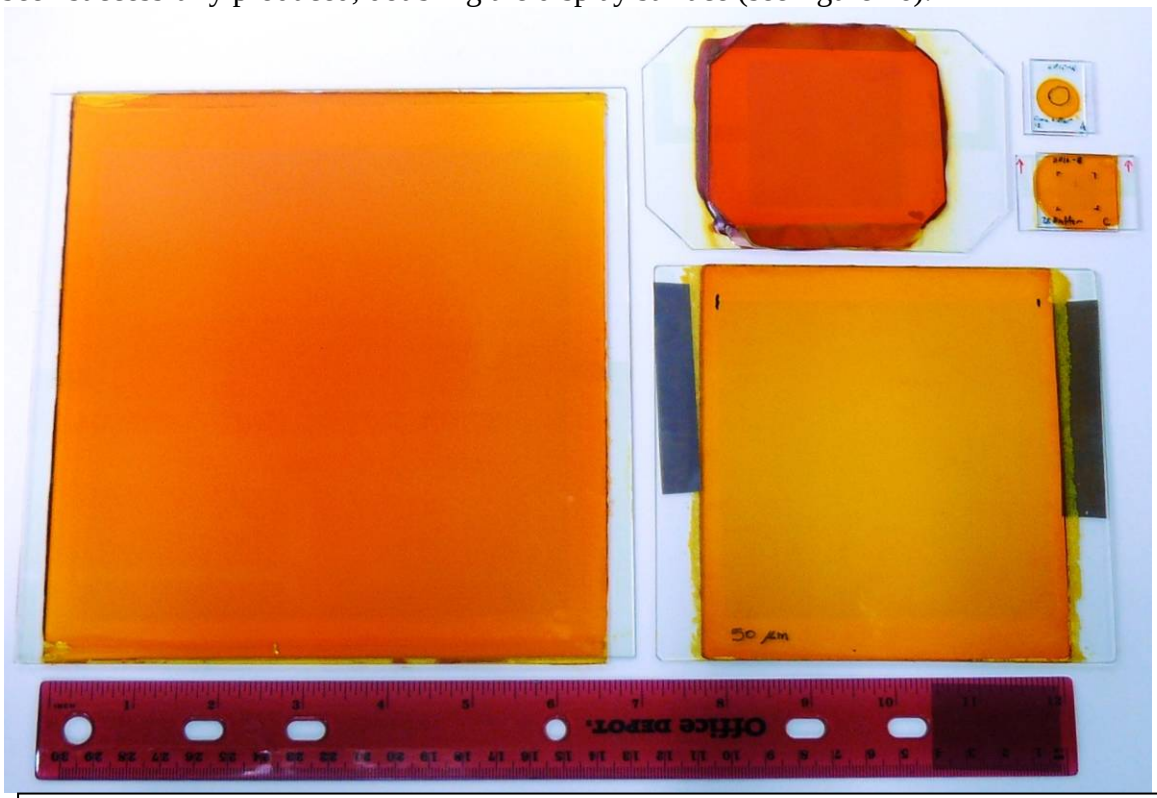

Figure 16. Size progression between each sample generation. From top right to left: small sample for 4 wave mixing characterization, 0.5 × 0.5 inch sample for image recording, 2 × 2 inches sample for 3D display first hologram, 4 × 4 inch sample for 3D display, and 6 × 6 inches sample.

A limit in the manufacturing technique has been reached with the 6 × 6 inch size. So far, the samples were made by casting the polymer between two glass plates. But with increasing size, inhomogeneities and inclusions are not well controlled and become a limiting factor for the display. Several samples experienced electrical break down due to these problems.

Figure 17. Sample manufacturing by vacuum lamination process**.** a. an ITO coated glass is spin coated with an APC buffer layer. b. a layer of active polymer is knife coated on the top of the electrode. c. Two coated glasses are assembled by hot pressing under vacuum ensuring good sample homogeneity.

A new technique is under development using a vacuum lamination chamber to assemble two pre-coated half-samples. First tests have shown good results on 6 × 6 inches samples (Fig.17) and the setup has been adapted to a maximum size of 1ft × 1ft.

Summary of work done by sub-contractors

1. Contribution to the final report

By Oksana Ostroverkhova

Objectives: 1) to develop a model describing space-charge field formation in an unsensitized photorefractive composite; 2) to understand properties of a buffer layer and its effects on photoconductivity and on the space-charge field dynamics; 3) to model an experimentally observed "voltage kick-off" effect, which is a speed-up in grating formation dynamics by applying a higher voltage for a short time prior to grating recording.

Outcomes: 1) demonstrated hole transport in the amorphous polycarbonate (APC) buffer layer, 2) established possibility of bipolar charge transport in the unsensitized photorefractive composite upon photoexcitation of FDCST chromophore, 3) modeled space-charge field steady-state and dynamics for various situations that qualitatively reproduce experimental results.

Results:

1. **Experimental**

(a) Cw photocurrent dynamics as a function of light intensity and applied voltage in ITO/APC/composite/APC/ITO and Al/APC/CuPc/ITO samples.

Measurements: Voltage is gradually ramped up (in order to reduce sample damage), and dark current is measured as a function of time using Keithley 2437 source-measure unit.

After about 100-150 s, a shutter is opened for 150-200 s, and a total current under 532-nm cw light is monitored. Finally, the shutter is turned off, and current relaxation down to a level of dark current is recorded. The experiment is repeated at different voltages and light intensities

(i) ITO/APC/composite/APC/ITO samples (Fig.18)

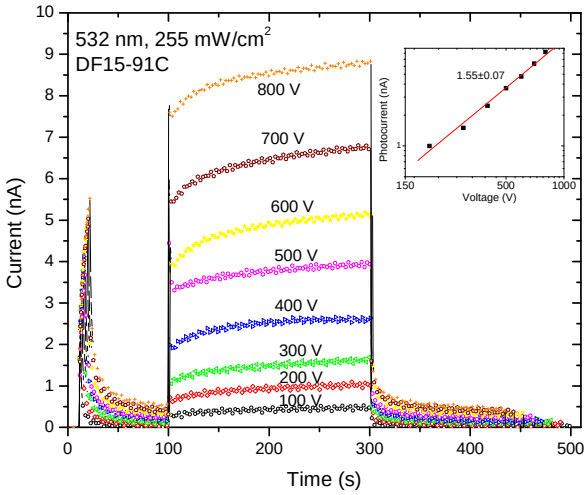

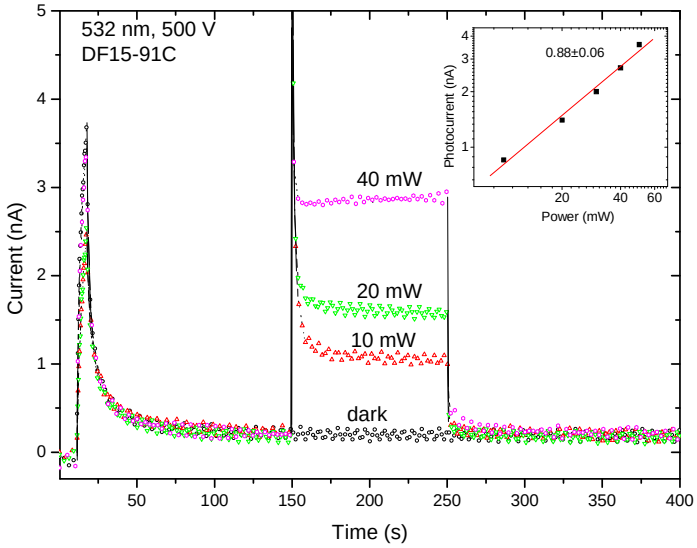

Figure 18. (a) Current dynamics at various applied voltages. At 10 s, voltage is ramped up. At 100 s, light beam is opened with a shutter, and photocurrent develops. At 300 s, the shutter is closed. Inset shows voltage dependence of the steady-state photocurrent (symbols) and a power-law fit (line), $I_{ph} \sim V^{a}$, with a = 1.55±0.07. (b) Current dynamics at various levels of light power. Light is turned on at 150 s and turned off at 250 s. Inset shows a power-law fit of the steady-state photocurrent values as a function of light power (intensity), $I_{ph} \sim I^{b}$, with b = 0.88±0.06.

Analysis:
Strong polarization current was observed due to polarizing of the APC molecules. The photocurrent dynamics are similar to those in typical PVK-based photorefractive composites. Super-linear voltage dependence of the photocurrent, due to that of photogeneration efficiency and mobility, is observed. Sub-linear light intensity dependence is consistent with the presence of shallow traps.

(ii) Al/APC/CuPc/ITO samples (Fig.19)

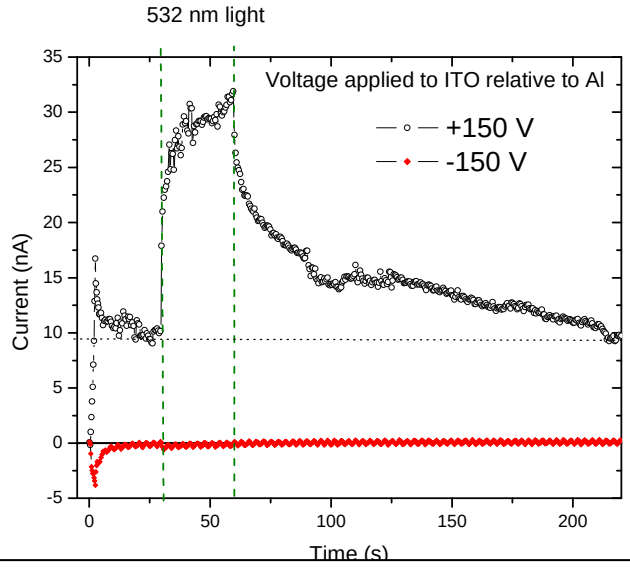

Figure 19. Long-time-scale current dynamics at two voltage polarities at the same 532-nm light intensity.

Analysis:
Asymmetry in both dark and photocurrent with respect to voltage polarity is observed, which is consistent with hole transport favored over electron transport in the CuPc and APC layers. Long decay of the photocurrent at +150 V was observed after the light was turned off, due to hole detrapping from deep traps in the APC layer, with subsequent discharging at the Al electrode.

(b) Time-of-flight experiments
Measurements: voltage was applied to a sample, and 355-nm 500-ps laser pulse excited charge carriers. Current due to carriers moving under electric field was measured. The following samples were tested: ITO/copolymer(80%)-ECZ(20%)/ITO, ITO/copolymer(50%)-FDCST(30%)-ECZ(20%)/ITO, and Al/APC/CuPc/ITO. Dispersive transients were observed in all samples, and carrier mobility could not be determined.

(c) Gap-scan experiments
Measurements: Samples are deposited on coplanar electrodes separated by a 15-25 μm gap. The sample is excited through a 10x microscope objective with a localized 532-nm beam, and

photocurrent is measured using lock-in amplifier, while scanning the beam spot across the gap. Samples tested included PDCST, PDCST/PMMA, PDCST/PVK, and copolymer/FDCST.

Results (Fig.20):

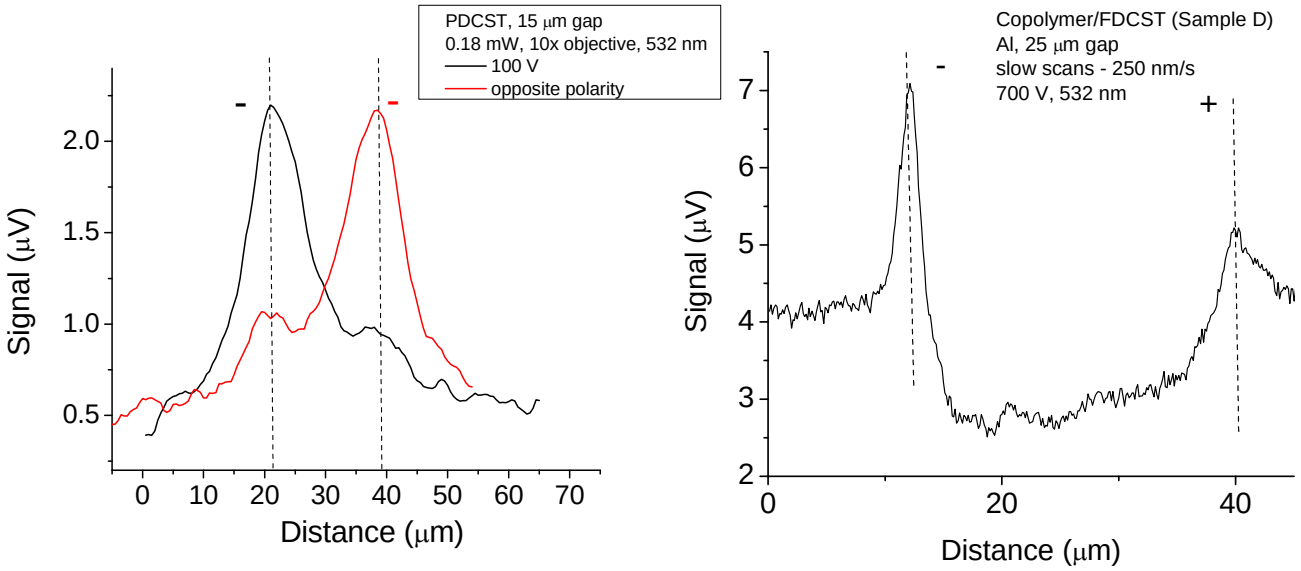

Figure 20. Photocurrent produced by a localized 532-nm excitation of (a) PDCST sample and (b) Copolymer/FDCST sample.

Analysis:

Our previous work with anthradithiophene derivatives which favor hole transport showed that in the gap scan experiments the photocurrent was highest when excited close to the positive electrode. Since the opposite is true for a PDCST dye film (Fig.20(a)), it may indicate that photogenerated electron transport is favored in pristine DCST films. Then, both hole and electron transport could be expected in a photorefractive composite containing hole-transporting copolymer and electron transporting DCST dye, which is supported by data in Fig.20(b).

2. Numerical simulations

Space-charge field formation and decay dynamics were simulated using several models. A simplest model that qualitatively reproduced experimental results from two-beam coupling, four-wave mixing, and photocurrent measurements is the following:

(i) Regular composite without buffer layers: chromophore is photoexcited; both holes and electrons are mobile; both hole and electron traps are taken into account.

(ii) Regular composite/buffer layers: deeper traps, fewer hole traps are available as compared to the sample without buffer layers.

(iii) Composite with PCBM: additional charge generation mechanism due to excitation of PCBM is taken into account; additional trap levels due to PCBM are introduced.

Results:

(a) Imaginary part of the space charge field (Im Esc) is directly related to an experimentally measured two-beam coupling gain coefficient. Figure 21 shows relative dynamics of the Im E_{sc} during the photorefractive grating formation. The differences in steady-state values of Im E_{sc} in composites with and without PCBM and with and without buffer layers are due to relative interplay of available trap concentrations and their depths. With particular combinations of trap parameters, experimental results are qualitatively reproduced. These include a change in energy transfer direction in a regular composite as buffer layers are introduced and changes due to addition of PCBM, both without and with buffer layers (Fig.21).

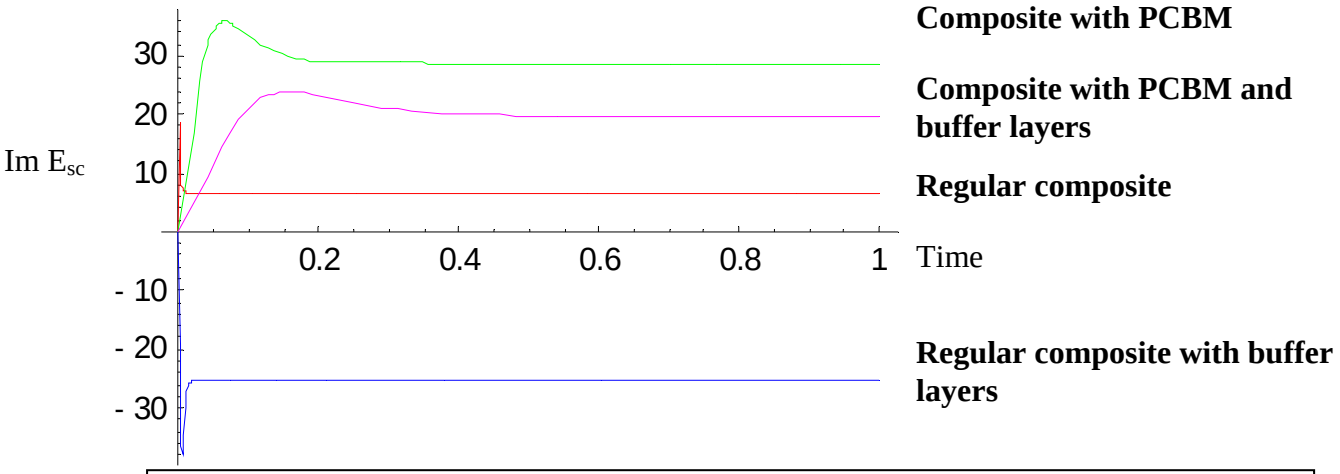

Figure 21. Imaginary part of the space-charge field as a function of time for regular composite without and with buffer layers (red and blue, respectively) and for PCBM-containing composite without and with buffer layers (green and magenta, respectively).

(b) Figure 22 shows decay dynamics of the square of the space-charge field (directly related to experimentally measured diffraction efficiency) in a regular composite sample with and without buffer layers. Due to changes in trapping properties (same as those used above for simulations of Im E_{sc}), decay dynamics in a sample with buffer layers are much slower, which reproduces experimental results.

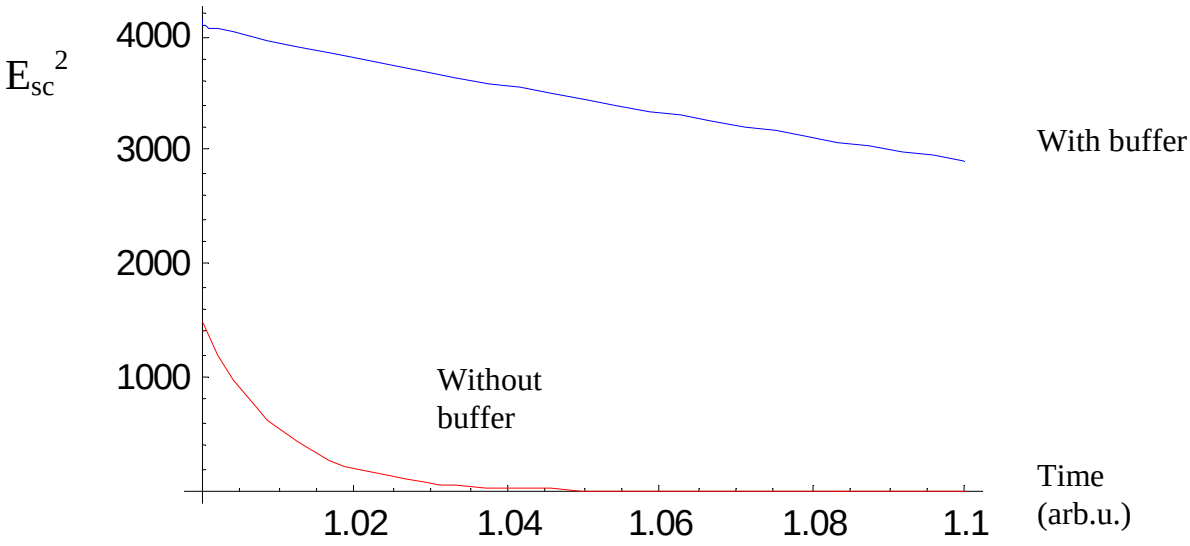

Figure 22. Dark decay of the square of the space-charge field in the regular composite with and without buffer layers (blue and red, respectively).

(c) Figure 23 shows a voltage kick-off effect, which is a speed-up of the grating formation dynamics by applying a higher "kick-off" voltage followed by its reduction to operating levels. The effect is achieved by charge generation and trap pre-filling during the kick-off pulse.

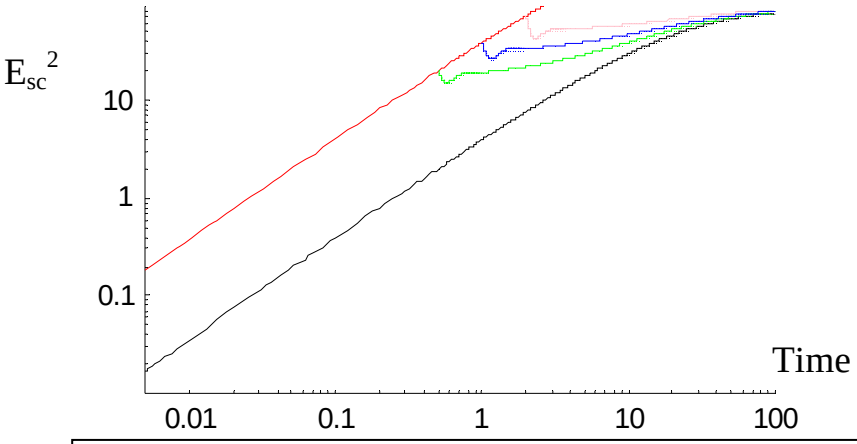

Figure 23. Grating formation dynamics with no "kick-off" (black), during the "kick-off" (red), and after the "kick-off", as the voltage is back to 4 kV, if the "kick-off" lasted for 0.5 s (green), 1 s (blue), and 2 s (pink). With the "kick-off", the steady-state diffraction efficiency is reached between one and two orders of magnitude faster than without the "kick-off".

2. **Contribution from Marder Group**

Our efforts have been largely focused on the development of new polymers as potential hole-transport materials, with possible applications in photorefractive composites. Since poly(*N*-vinylcarbazole) (PVK) is one of the most widely used hole-transporting hosts for photorefractive composites, we have synthesized a wide range of new carbazole-based polymers based on a poly(norbornene) backbone using ring-opening metathesis polymerization (ROMP). Representative examples of the structures synthesized are shown in Fig. 24. In each of the cases shown, a carbazole-functionalized alcohol was esterified with 5-norbornene-2-carboxylic acid to give the monomer, which was then polymerized using one of the ruthenium-based initiators developed by Grubbs.

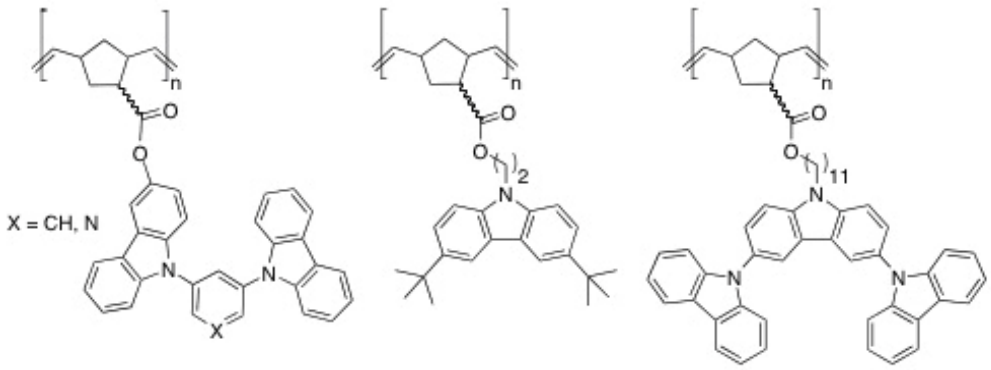

Figure 24. Carbazole-based hole-transport polymers synthesized using ROMP.

One advantage of ROMP is that it offers good control over the polymer molecular weight, perhaps thereby enabling us to tune morphological and rheological properties such as the glass-transition temperature, thus obviating the need for addition of plasticizers to the composites. For example, in the preparation of the polymer used on the left-hand side of Fig. 24 in which X = CH, use of 1 mol% ruthenium initiator ("Grubbs 1st generation") led to a polymer with a reasonably narrow polydisperisity index of 1.3 and a a degree of polymerization of ca. 64, only falling a little short of the target value of 100. Moreover, ROMP is tolerant of a wide-range of functional groups, thus offering the possibility for copolymerization of the hole-transport monomer with sensitizer- and / or chromophore-functionalized norbornene monomers. Indeed, in work funded from other sources, we have used copolymerized of these monomers with monomers with electron-transport or luminescent functionality for use in organic light-emitting diodes (OLEDs). To illustrate the flexibility of this approach, we have used a variety of carbazole-based monomers. These include carbazoles with 3,6-susbtituents (*tert*-butyl groups

and additional carbazol-9-yl groups), in contrast to the irreversible behavior of PVK and other carbazoles due to reaction of the corresponding radical cations through these positions, these materials exhibit reversible first oxidations; we anticipate that this feature could potentially improve the long-term stability of carbazole-based photorefractives. In particular, the use of the tricarbazole group is inspired by the use of small molecules based on this moiety as hole-transport and host materials for phosphors in OLEDs. Indeed we have found (in work funded by other sources) that the polymer can be used as both host and hole-transport layer in OLEDs, this demonstrating that the norbornene backbone does not interfere with the hole-transport behavior of these polymers.